A search for gravitational waves from the millisecond pulsar PSR 0437-471

S. D. Mohanty[†*], I. S. Heng, D. G. Blair, S. V. Dhurandhar[†], M. Tobar, E. Ivanov

Dept. of Physics, University of Western Australia, Nedlands, WA 6009, Australia.

[†] *IUCAA, Post Bag-4, Ganeshkhind, Pune 411 007, India.*

Abstract

A search for gravitational waves from the millisecond pulsar PSR 0437-471 has been initiated using the bar detector NIOBE which is located at the University of Western Australia. This search involves a very long coherent integration of the bar output which may stretch over a few years. We present a detailed report on the data analysis algorithm, called *phase plane rotation*, which will be used in this search. A discussion of the actual implementation of the algorithm is presented.

Key words: gravitational waves, milli-second pulsars, resonant bar detectors.

*Present address: LIGO Project, MS 18-34, California Institute of Technology, Pasadena, CA 91101, U.S.A.

I. INTRODUCTION

Pulsars with non-axisymmetric deformations will radiate a part of their rotational kinetic energy in gravitational waves. If the signal phase is known, either from electromagnetic observations in the case of a known pulsar or as a parametrised model in the case of a survey for unknown ones, a coherent integration of the detector output can be employed to enhance the signal to noise ratio. An integration involving electromagnetic observations as input is called a *targeted* search. A survey for the detection of unknown pulsars, called an *all sky - all frequency* search, uses a model of the signal which is parametrised by the frequency, frequency derivatives and angular position of the pulsar.

An all sky-all frequency search for pulsars appears, at present, to be a daunting task computationally (Brady et al. 1997) even for isolated pulsars, let alone pulsars in binaries. On the other hand, a targeted search for signals from known pulsars would be computationally possible. Such a search can handle binary pulsars as well as isolated ones and can even handle pulsar glitches. However, estimates of the gravitational wave strain h expected from known pulsars lie around 10^{-25} or less. To detect such a signal with the current sensitivities of detectors, or even with more advanced ones in the future, a coherent integration stretching over a year or more would be required.

A series of such attempts, using succesively more sensitive resonant mass detectors, have already been performed by the group at Tokyo (Tsubono 1991; Owa 1986; Owa et al. 1988). This experiment sought a quadrupolar signal from the Crab Pulsar at twice its rotational frequency. Special purpose resonant mass antennae were built with a low resonant frequency of $\sim$ 60 Hz. The resonant frequency was electrostatically tuned to track the pulsar frequency as it drifted due to doppler shifts. The integration period was $\sim$ 1000 hrs for the Crab III experiment, the third one in the series.

The normally dominant mode of gravitational wave radiation from a pulsar would be quadrupolar, at twice its rotational frequency. This was the reason behind the choice of the resonant frequency in the Tokyo experiment. However, there should be radiation at other

harmonics also in general. By a fortuitous coincidence, the fourth multiple of the rotational frequency of the millisecond pulsar PSR 0437-471 (Johnston et al. 1993; Sandhu et al. 1997) happens to lie within the bandwidth of one of the resonant modes of NIOBE, the resonant bar gravitational wave detector at the University of Western Australia. PSR 0437-471 has a rotational period of 5.75 msec and lies at a distance of ~ 178 pc (the dispersion measured derived distance is 140 pc). It forms a binary with a white dwarf, the orbital period being 5.74 days. The spin down luminosity of the pulsar is $\sim 10^{34}$ ergs/sec.

A formalism for wave generation that is appropriate for slowly moving but strong field sources, such as pulsars, was given by Ipser (Ipser 1971). Using this formalism, an upper bound to the r.m.s. gravitational wave strain h can be obtained by assuming that the spin down of a pulsar is entirely due to gravitational wave radiation. In the case of PSR 0437-471, if the radiation is assumed to be entirely at the fourth multiple alone, we get $h \sim 10^{-26}$ (Dhurandhar et al. 1996 (henceforth referred to as paper I)). With an enhancement in sensitivity (Blair et al. 1995) of the detector, planned for the near future, it would take about 3 years of coherent integration to detect a signal with the above r.m.s amplitude.

Even if the true situation were less favorable to detection, important lessons in data analysis can be learned from actually implementing such a long coherent integration. Such experiences may help more sensitive searches of the future, such as ones using the very long baseline laser interferometric detectors that are now under construction.

An algorithm for such a coherent integration, which we call *phase plane rotation* (PPR), was introduced by Dhurandhar, Blair and Costa in paper I. Though this algorithm is a variant of the well known technique of matched filtering, it has the advantage that it is well adapted to the already existing data aquisition facilities of bar detectors and needs no modifications in the hardware.

In this paper we report on the actual initiation of a coherent integration, using PPR, of the data from NIOBE. Important results from this very long integration, which may stretch over a few years, will be communicated in later works. We investigate the algorithm itself in greater detail and find that there are two parameters governing PPR whose effect was

ignored in the earlier analysis. One of the parameters is the inclination angle between the rotation axis of the pulsar and the line of sight to it. The other is the direction of the pulsar spin vector projected on the plane of the sky. Both these parameters are determined poorly by radio observations and, hence, the phase obtained from radio is not complete. We also discuss practical issues involved in the implemenation of this algorithm.

We begin with a review of PPR in Section II. Some notation and typical numbers are also introduced in this section. The behaviour of noise under phase plane rotation is investigated in Section III. In Section IV, we describe the signal wave form. The effect of polarization phase on the signal to noise ratio (SNR) is investigated in Section V. Details of an actual implementation of the algorithm are described in Section VI. We conclude with Section VII.

II. A BRIEF REVIEW OF THE PHASE PLANE ROTATION SCHEME

The resonant bar detector NIOBE is a two mode system consisting of a primary mass, which is a 2.75 m long Niobium bar with an effective mass of 700 Kg, and a smaller secondary mass attached to it. The quantity which is measured is the longitudinal motion of the secondary mass using an electro-mechanical transducer.

The normal modes of the detector that are relevant to gravitational wave detection have frequencies denoted by f_+ and f_- with $f_+ \simeq 700.1$ Hz and $f_- \simeq 694.5$ Hz. The fourth multiple of the rotational frequency of PSR 0437-471 is at 694.75 Hz which lies close to f_-. Henceforth, we will be concerned with this mode only. We denote the frequency of the fourth multiple by f_p, where $f_p = 694.75$ Hz.

The output of the transducer is amplified and processed through a lock-in amplifier. If the input to the lock-in be $x(t)$ then there are two outputs $X(t)$ and $Y(t)$,

$$X(t) = \int_{-\infty}^{\infty} dt' K_L(t-t') x(t) \cos(\omega_{\rm ref} t + \phi_l) \,, \tag{1}$$

$$Y(t) = -\int_{-\infty}^{\infty} dt' K_L(t-t') x(t) \sin(\omega_{\rm ref} t + \phi_l) \,, \tag{2}$$

where, $K_L(x)$ is the transfer function of a low pass filter ($K_L(x) = 0$ for $x < 0$), $\omega_{\rm ref} = 2\pi f_{\rm ref}$ is the angular frequency of the reference signal used in the lock-in and ϕ_l is the phase of the

reference signal at some fiducial instant. The negative sign in the case of $Y(t)$ is used for consistency with the analysis of paper I.

In a comoving frame, the signal from PSR 0437-471 would be nearly monochromatic apart from a small spin down ($\dot{P} \sim 10^{-20}$ sec/sec). But at the detector this monochromatic signal is spread over a bandwidth of ~ 0.1 Hz due to doppler shifts produced by the motion of the pulsar in its binary orbit and the rotational and orbital motion of the Earth.

Thus, the signal $s(t)$ in the detector output would be a narrow band signal which can be represented as,

$$s(t) = A(t)\cos(\theta(t)) \ . \tag{3}$$

The lock-in outputs corresponding to $s(t)$ would be,

$$X(t) = A(t)\cos\left[\theta(t) - \omega_{\rm ref}t - \phi_l\right] \ , \tag{4}$$

$$Y(t) = A(t)\sin\left[\theta(t) - \omega_{\rm ref}t - \phi_l\right] \ . \tag{5}$$

The value of $f_{\rm ref}$ is kept near f_-. The action of the lock-in, therefore, is to heterodyne the detector output and produce the two quadrature components of a phase modulated signal.

The instantaneous output of the lock-in can be thought of as a vector (X, Y) in some phase plane and the vector $\left(\int^t X(t')dt', \int^t Y(t')dt'\right)$ as the path traced out in this phase plane by the lock-in output. The phase plane rotation scheme consists of making the following instantaneous transformation on (X, Y),

$$X'(t) = X(t)\cos\left[\theta_R(t)\right] + Y(t)\sin\left[\theta_R(t)\right] \ , \tag{6}$$

$$Y'(t) = -X(t)\sin\left[\theta_R(t)\right] + Y(t)\cos\left[\theta_R(t)\right] \ , \tag{7}$$

where,

$$\theta_R(t) = \theta(t) - \omega_{\rm ref}t - \phi_l \ . \tag{8}$$

This is a rotational transformation which can be thought of as either rotating the phase plane by $\theta_R(t)$ or the vector (X, Y) by $-\theta_R(t)$. It is understood here that the rotation is

by an angle $\theta_R(t)$ upto some unknown but constant offset present in the gravitational wave signal.

From Eqs. (4), (5) and Eqs. (6), (7), it follows that in the rotating plane (X', Y'), the signal vector will point in the same direction at all times. On the other hand, the noise vector will have a random orientation. Thus, the displacement of the signal path will grow at a faster rate than that of the noise and a detection can be made by computing the probability that the observed final displacement could have arisen due to noise alone. The detection statistic, therefore, is the length of the final displacement of the output path from the origin.

We show in Appendix A that the signal to noise ratio (SNR) achieved by PPR is almost the same as that obtained using matched filtering on the detector output $x(t)$. If the signal is assumed to be approximately monochromatic, the signal to noise ratio (SNR) that can be achieved by matched filtering over an integration period T can be expressed as,

$$SNR \simeq \frac{\sqrt{T}A}{\sqrt{S_n(f_s)}}, \tag{9}$$

where $S_n(f)$ is the two sided strain noise power spectral density, f_s the signal frequency and A its r.m.s. amplitude.

If all the spin-down luminosity of PSR 0437-471 is in gravitational radiation at the frequency f_p, then $A \sim 10^{-26}$ (in terms of the strain produced by the wave (see paper I)). An $SNR = 1.6$ (which implies detection at an 80% confidence level) would then be obtained, at the present sensitivity of the antenna, for $T \sim 10^{10}$ sec. For the planned enhancement in sensitivity (Blair et al. 1995), the integration time would fall to $T \sim 10^8$ sec. The above estimates assume the noise to be stationary. In practice, this is only approximately true and the actual integration time required may be somewhat higher.

III. THE BEHAVIOUR OF NOISE IN PHASE PLANE ROTATION

The noise in the detector output consist of two components with very different auto-correlation times. In a simple model of the detector (Pallatino & Pizzella 1991), the Brownian motion of the fundamental mode and the back action noise of the transducer are

filtered through the bar transfer function to emerge as narrow band noise with a large auto-correlation time. To this the amplifier adds wide band noise which is almost white, and hence, has a short auto-correlation time. We denote the corresponding noise components in the outputs of the lock-in by X_{nb} (Y_{nb}) for the narrow band and X_{wb} (Y_{wb}) for the wide band noise.

The narrow band noise X_{nb} is centered around the mode frequency f_- and can be represented as,

$$X'_n(t) = A_n(t)\cos[2\pi f_- t + \phi_n(t)] \; . \tag{10}$$

Y_{nb} can also be represented similarly. It is easy to show, using this representation and Eqs. (6) and (7), that in the rotating plane, the vector $(X_{nb}(t), Y_{nb}(t))$ is rotated by an angle $2\pi f_- t - \theta(t)$.

Thus, if the rotational period of the phase plane, $1/(f_- - f_p)$, is much smaller than the auto-correlation time of the narrow band component, the path of this component in the rotating plane would be a circular motion around a randomly moving centre. The wide band component should, on the other hand, execute a random walk similar to its behaviour in the non-rotating plane. Thus, the overall effect is to produce a circularly "smeared" random walk.

We illustrate this in Fig 1. This figure shows the path followed by 15 min of real data in the rotating plane, where the rotational transformation used corresponds to a monochromatic signal with a frequency f_s such that $f_s - f_- = 0.2$ Hz. This is the least offset in frequency that the pulsar signal is expected to have from f_- (see paper I). In this figure the solid line represents the path followed by wide band noise alone while the path followed by the total noise is shown by dots. The circular smearing effect due to the narrow band noise is evident. We have separated out the two noise components by low pass filtering the data with an arbitrary cut off frequency. Thus, the wide band component shown in the figure should be understood as only an approximation to the actual one.

In Fig 2, we show the same data as in Fig 1 but with a monochromatic signal having the

same phase as used in the rotational transformation, apart from a constant offset, added to it prior to transformation. This shows how, under PPR, the path followed by the output acquires a systematic deviation in the direction of the signal vector.

IV. THE SIGNAL

In the following we will use the celestial coordinate system based on the equator and equinox of date to give the angular positions of the detector as well as the pulsar.

In the transverse traceless (TT) gauge with the z-axis along the direction of wave propagation (*wave frame*), a gravitational wave signal is represented by two components $h_+(t)$ and $h_\times(t)$. Let the X axis in the wave frame be oriented along the projection of the pulsar's spin axis on the sky plane. The components h_+ and $h_\times$ can be expressed (Thorne 1987) in this choice of axes as,

$$h_+(t) = h_0(1 + \cos^2 i)\cos[\theta_s(t)] \ , \tag{11}$$

$$h_\times(t) = 2h_0 \cos i \sin[\theta_s(t)] \ , \tag{12}$$

where h_0 depends on the distance to the pulsar and the structure of the deviations from axisymmetry in the pulsar, i is the angle at which the rotation axis of the pulsar is inclined to the line of sight and $\theta_s(t)$ is the phase of the pulsar signal at the site of the detector.

When $i = 0$, the radiation is circularly polarized and it is linearly polarized when $i = \pi/2$. In the case of PSR 0437-471, $\theta_s(t)$ can be obtained directly on the basis of radio pulse timing observations. A sequence of pulse arrival times yield the orbital parameters of the binary which can then be used to predict the signal phase.

The fundamental mode of the bar (the one which is relevant here, namely, f_-) can be modeled as a damped multiple oscillator driven by the incident gravitational radiation. The driving force $F(t)$ is given by (Dhurandhar & Tinto 1988),

$$F(t) = F_+\ddot{h}_+ + F_\times\ddot{h}_\times \ , \tag{13}$$

where, F_+ and $F_\times$ are the antenna beam patterns given below.

The response of the bar $\xi(t)$ (displacement measured by transducer) can be obtained in the Fourier domain as,

$$\tilde{\xi}(\omega) \propto \frac{1}{(\omega_m^2 - \omega^2) - 2i\frac{\omega}{\tau}} \tilde{F}(\omega) \ , \tag{14}$$

where τ is the integration time of the transfer function associated with the mode. For the mode f_-, $\tau \sim 50$ sec.

The functions F_+ and $F_\times$ can be expressed as,

$$F_+ = F'_+ \cos\psi - F'_\times \sin\psi \ , \tag{15}$$

$$F_\times = F'_\times \sin\psi + F'_+ \cos\psi \ , \tag{16}$$

where, F'_+ and $F'_\times$ are the antenna patterns for a specific choice of the wave X-Y axes orientation, namely, X axis pointing towards the celestial South pole and Y axis towards the West. ψ is the angle between this X axis and that of the preferred wave frame in which Eqs. (11) and Eq. (12) are obtained.

Let (α, β) be the coordinates of the detector and (θ, ϕ) be that for the source. Then, F'_+ and $F'_\times$ are expressed as,

$$F'_+ = n_1^2 \cos^2\theta - 2n_1 n_3 \cos\theta \sin\theta - n_2^2 + n_3^2 \sin^2\theta \ , \tag{17}$$

$$F'_\times = 2n_1 n_2 \cos\theta - 2n_2 n_3 \sin\theta \ , \tag{18}$$

where,

$$n_1 = \cos\alpha \cos\beta \cos\gamma - \sin\beta \sin\gamma \ , \tag{19}$$

$$n_2 = \cos\alpha \sin\beta \cos\gamma + \cos\beta \sin\gamma \ , \tag{20}$$

$$n_3 = -\sin\alpha \cos\gamma \ . \tag{21}$$

Note that since β is time dependent, both F_+ and $F_\times$ are time dependent functions.

We show in Appendix B that, because of the short integration time τ in Eq. (14), the phase of the response $\xi(t)$ has a nearly constant offset from the phase of the force $F(t)$. We denote this phase offset by Φ_b. We can, therefore, express $\xi(t)$ as,

$$\xi(t) = A_s(t)\cos(\theta(t) + \Phi_b)\ , \tag{22}$$

where,

$$A_s(t) = kh_0\theta_s^2\left(1+\cos^2 i\right)\left[F_+^2 + (F_\times\rho)^2\right]^{1/2}\ , \tag{23}$$

$$\theta(t) = \theta_s(t) + \Phi_P(t;\ \psi,\rho)\ , \tag{24}$$

$$\Phi_P(t;\ \rho,\psi) = \tan^{-1}\left[\tan\left(2\psi + \tan^{-1}\frac{F'_\times}{F'_+}\right)\rho\right]\ , \tag{25}$$

$$\rho = \frac{2\cos i}{1+\cos^2 i}\ . \tag{26}$$

The above expressions are obtained under the approximation $\ddot{\theta}_s \ll \dot{\theta}_s$. In the case of PSR 0437-471, $\ddot{\theta}_s \sim 10^{-6}$ Hz/sec while $\dot{\theta}_s \simeq f_p$ and, hence, the approximation is valid. The constant k comes from the bar transfer function. The term $\Phi_P(t;\ \rho,\psi)$ is called *polarization phase* (Cutler 1997). Unlike θ_s, it is known only partially since the parameters ρ and ψ are difficult to deduce from radio observations.

In Fig. 3, we plot the polarization phase of PSR 0437-471 for several values of ρ at $\psi = 0$. As can be seen from the figure, polarization phase varies over a wide range and cannot be neglected in any detection scheme, like matched filtering or PPR, which integrates the signal coherently.

V. THE EFFECT OF ρ AND ψ ON SIGNAL TO NOISE RATIO

As mentioned earlier, the values of ρ and ψ are not fixed by radio observations. In the following, we denote the values of ρ and ψ used to perform a rotational transformation by $\widehat{\rho}$ and $\widehat{\psi}$. The values of these parameters in the signal wave form will be denoted by ρ_s and ψ_s.

In the case of a mismatch between the signal and transformation parameter values, the transformed signal path will wander in the phase plane and the detectability of the signal will suffer. Thus, in general, integrations with different values of $\widehat{\rho}$ and $\widehat{\psi}$ must be used in order to reduce the amount of mismatch for any signal. This is analogous to the bank of templates required in the case of coalescing binary signals.

What criterion should be adopted in order to fix the bank of integration parameters? Consider the following facts. The lifetime of this experiment, though long, would still be limited because of practical reasons. Now, the shortest integration period required for a given signal depends on the values of its parameters. When the signal and transformation parameters match exactly, the displacement of the signal path is $\int_0^T dt\, A_s(t)$, and it can be seen from Eq. 23 that $A_s(t)$ depends on ρ_s and ψ_s. It is easily shown that if the signal has $\rho_s = 1$, its integration period (when $\widehat{\rho} = 1$ and $\widehat{\psi} = \psi_s$) is the shortest among all other values of ρ_s, ψ_s. This is independent of the value of ψ_s when $\rho_s = 1$. We denote this minimum period by $T_{\rm min}$.

If it were possible to obtain $T_{\rm min}$ *a priori*, one could fix the lifetime of the experiment. For instance, it can be kept at, say, $\sim 2T_{\rm min}$ so that more unfavourable signal parameter values can also be detected. However, since the overall amplitude of the signal h_0 (see Eq. (23)) is unknown, the absolute value of $T_{\rm min}$ cannot be obtained. However, though the absolute value of $T_{\rm min}$ is unknown, it is quite legitimate to adopt a criterion based on *relative* comparision with $T_{\rm min}$. We, therefore, demand that the bank of transformation parameters be chosen in such a way that the integration period required for a signal be not more than twice that which is required when $\rho_s = 1$ and $\widehat{\rho} = 1$, $\widehat{\psi} = \psi_s$.

It is possible that for some values of ρ_s and ψ_s, a signal may pass undetected in the limited lifetime of the experiment, even if an integration with exactly matching parameters were used. The size of such a region of "undetectability" in parameter space will depend on the value of h_0. In the case of PSR 0437-471, radio observations as well as the present evolutionary model for the binary system (Bailes 1997) suggest that $\rho_s \sim 1$. Thus, the signal parameters may not be unfavourable in this case.

Having adopted the above criterion, we proceed to fix the bank of integration parameters as follows. The SNR obtained in an integration period T is proportional to $L/\sqrt{T}$ where, L is the displacement of the signal path from the origin in that period. Now, since all terms occurring in the polarization phase have a periodicity of 24 hours, we need to estimate the reduction in SNR over an integration period of 24 hours only. Therefore, we need the

displacement of the signal path from the origin over an integration period of 24 hours. We denote this quantity by $L(\widehat{\rho}, \widehat{\psi};\, \rho_s, \psi_s)$,

$$L(\widehat{\rho}, \widehat{\psi};\, \rho_s, \psi_s) = \left[\left(\int_0^{T'} dt\, A_s(t) \cos[\Phi_P(t;\, \rho_s, \psi_s) - \Phi_P(t;\, \widehat{\rho}), \widehat{\psi}] \right)^2 + \left(\int_0^{T'} dt\, A_s(t) \sin[\Phi_P(t;\, \rho_s, \psi_s) - \Phi_P(t;\, \widehat{\rho}, \widehat{\psi})] \right)^2 \right]^{1/2}, \tag{27}$$

where $T' = 24$ hours.

The maximum value of $L(\widehat{\rho}, \widehat{\psi};\, \rho_s, \psi_s)$ is obtained when $\widehat{\rho} = \rho_s$, $\widehat{\psi} = \psi_s$ and $\rho_s = 1$. We denote this value by $L_{\max}$. As mentioned earlier, the integration period in this case is $T_{\min}$. Now let,

$$\epsilon(\widehat{\rho}, \widehat{\psi};\, \rho_s, \psi_s) = \frac{L(\widehat{\rho}, \widehat{\psi};\, \rho_s, \psi_s)}{L_{\max}}\,. \tag{28}$$

From the dependence of SNR on L and T, it is easily seen that when there is a mismatch between signal and transformation parameters, the time required to achieve the same SNR would be $T_{\min}/\epsilon(\widehat{\rho}, \widehat{\psi};\, \rho_s, \psi_s)^2$. Hence, if we require the integration period of a signal to not exceed $2T_{\min}$ in the case of a mismatch, we should have at least one integration with $\widehat{\rho}$ and $\widehat{\psi}$ such that $\epsilon(\widehat{\rho}, \widehat{\psi};\, \rho_s, \psi_s) \geq 0.71$.

We have plotted, in Fig. 4, the contours of $\epsilon(\widehat{\rho}, \widehat{\psi};\, \rho_s, \psi_s)$ as a function of $\widehat{\rho}$ and $\widehat{\psi}$ for a pulsar inclination angle $i = 30°$ (corresponding to $\rho_s = 0.9897$) and $\psi_s = 20°$. We see that in this case the $\epsilon(\widehat{\rho}, \widehat{\psi};\, \rho_s, \psi_s)$ surface is quite flat (though there does exist a weak local maximum at $\widehat{\rho} = \rho_s$ and $\widehat{\psi} = \psi_s$). Hence in this case, it is sufficient to use $\widehat{\rho} = 1$ and $\widehat{\psi} = 0$ for the integration.

We find that the $\epsilon(\widehat{\rho}, \widehat{\psi};\, \rho_s, \psi_s)$ surface is likewise flat for $\rho_s \simeq 0.91$ or less and for all values of ψ_s. This range of ρ_s actually corresponds to a wide range of inclination angle since, for $\rho_s = 0.91$, the inclination angle $i \simeq 50°$. Beyond this value, an integration with $\widehat{\rho} = 1$ and $\widehat{\psi} = 0$ proves insufficient but so does an integration matching the signal parameters.

Thus, we conclude that, according to our criterion (i) signals with $i \geq 50°$ cannot be detected, (ii) for signals with $i \leq 50°$, it is sufficient to use a single transformation, namely,

$\widehat{\rho} = 1$, $\widehat{\psi} = 0$. It should be noted that $\epsilon(\widehat{\rho}, \widehat{\psi}; \rho_s, \psi_s)$ depends on the angular positions and orientation of NIOBE and PSR 0437-471. Our conclusions above are, therefore, specific to this case.

VI. IMPLEMENTATION OF THE ALGORITHM AND RESULTS

The algorithm is implemented within a MATLAB environment with some modules written in FORTRAN. The integration is performed off-line on recorded data at intervals of, usually, a week. The data consists of 15 minutes segments with each of the lock-in outputs X and Y recorded separately. The two quadratures are sampled with a frequency of 10 Hz with a 15 bit quantization of the amplitude.

The pulsar phase $\theta_s(t)$ is obtained by making piecewise polynomial fits over intervals of one day. The polynomial coefficients are obtained using the program TEMPO (Taylor & Weisberg 1989). The pulsar phase is generated as a function of Universal time (UT1) while the data is time-stamped using Coordinated Universal time (UTC). We convert the UTC time instants to UT1 using the solution C04 provided by the International Earth Rotation Service (IERS www site).

C04 tabulates the difference $DUTC = UT1 - UTC$ at intervals of a day. The sub-diurnal variations in $DUTC$ can be accounted for in our case by a simple linear interpolation. However, we use the more accurate program INTERP which codes Ray's model [7]. The UTC time stamps are obtained by synchronizing the laboratory clock with GPS. The accuracy in the UT1 time stamp is $\sim 10^{-5}$ sec and it is $\sim 10^{-7}$ sec for the UTC time stamp. The angular position of the detector site, with respect to the equator and equinox of date, is obtained using the subroutine TERRA provided in the package NOVAS (Kaplan).

The software transforms the data using Eqs. (6) and (7), and the displacement vector of the output path is provided at 15 minute intervals. Before processing any segment of the data, its quality is checked with regard to unusually large fluctuations. In case the noise temperature of the data segments, as computed using the Zero Order Prediction (ZOP) (Pal-

latino & Pizzella 1991) algorithm, exceeds a preset threshold, that segment is rejected.

Whenever the detector is stopped and restarted, the lock-in reference signal phase is recorded. Also, the reference frequency is periodically checked and reset if a drift is observed. The phase at such times is also recorded. The mode frequency f_- and other parameters entering $\eta(\Delta\omega)$ (see Appendix B) can drift, though by very small amounts, and they are periodically checked and recorded. All such information is taken into account in the integration routines.

The error between the phase $\theta_R(t)$, used for the rotational transformation, and the actual phase that the signal may have will be dominated by the mismatch between the signal and transformation parameters ρ, ψ. However, in case the mismatch between them happens to be small, other sources of error may also become significant. Their effect should, therefore, be estimated.

We give here a list of possible sources of error in the phase apart from that due to parameter mismatch.

(i) Uncertainty in the pulsar phase $\Phi_s(t)$ obtained from electromagnetic observations : The phase $\Phi_s(t)$ is obtained using the program TEMPO. Since the integration is done on data which has already been recorded, we do not need a *prediction* for the phase but a past record. This is expected to have an average instantaneous accuracy of $\sim 1°$, in contrast to the accuracy of the *predicted* phase which worsens with time (Bailes 1997).

(ii) Error in the angular position of the source and the angular position and orientation of the bar : This source of error can, in principle, affect both $\Phi_s(t)$ and $\Phi_P(t)$. The bar's angular position has been obtained using the Global Positioning System (GPS) and is accurate to within a few arc seconds. The angular position and proper motion of the source are known to an extremely high accuracy (Sandhu et al. 1997). The effect of this source of error on both $\Phi_s(t)$ and $\Phi_P(t)$ is negligible.

(iii) Drifts in the physical parameters of the detector leading to a drift in ϕ_b : For instance,

the mode frequency f_- can change due to changes in the input power of the microwave transducer. The effect of such drifts is expected to be negligible and, moreover, they can be measured and necessary corrections made.

(iv) Phase noise in the lock-in reference signal : The quoted parameters for the instrument used to generate the reference frequency, a HP3325A wave form synthesizer, make this an extremely small error.

(v) Drift in reference frequency : Again a negligible source of error.

(vi) Accuracy in timing : errors in putting accurate time stamps for the data samples will induce errors in Φ_s, $\Phi_P(t)$ and $f_{ref}t$ used in the rotational transformation phase $\theta_R(t)$. As mentioned above, we synchronize our laboratory clock with UTC (coordinated Universal time) as transferred by GPS. UTC is based on International Atomic time with suitable semi-annual corrections that are added to keep it synchronized to UT1 (Universal time) (Seidelmann 1992). The values of DUTC in C04 are listed at intervals of one day while the change in DUTC over that interval is $\sim$ 2.0 msec. If this drift within a day is not taken into account, it can lead to a significant loss in SNR in our case. However, using the program INTERP, mentioned above, our UT1 time stamp should have an accuracy of $\sim$ 10 μsec at all epochs.

(vii) Numerical errors in the integration : We use double precision arithmetic with a precision of 15 decimal places which is more than sufficient to eliminate numerical errors in our case.

At the lowest order, the total error due to all the sources listed above would be just be a sum of all the individual errors. Thus, a fair estimate of the total instantaneous phase error due to the sources listed above is $\sim 1^\circ$ or less. As shown in Appendix C, this error is not serious if it is treated as a random error. However, some of the errors above would be systematic in nature and their effect must be considered more carefully.

One serious source of error could be error in the frequency of the lock-in reference signal. In the case of NIOBE, the lock-in reference signal is externally generated by an HP3325A wave form synthesizer. As of now the frequency accuracy of this instrument ($\pm 5 \times 10^{-6}$ of selected value) is inadequate for our purpose. However, this is a hardware problem which can be easily overcome by going over to a much more accurate instrument. This problem is under consideration at present.

VII. CONCLUSION

We have written numerical codes for implementing the *Phase Plane Rotation* algorithm (PPR) which was introduced in paper I. We have investigated the theory of this algorithm in more detail and made the earlier analysis more complete by incorporating and investigating the effect of polarization phase on the detection of the signal.

It was shown that polarization phase, which arises from the different amplitude modulations of h_+ and $h_\times$, depends on the parameter ρ and ψ whose values are not well determined by radio observations, unlike the phase of the pulsar radio pulse itself. However, we found that for the case of PSR 0437-4715 and NIOBE, the data needs to be transformed and integrated for only one value of ρ and that ψ does not affect the integration seriously. It should be investigated whether this is only true for the particular case of NIOBE and PSR 0437-4715 or it is true in general.

A number of practical issues were identified which are potentially important in the very long coherent integration that is going to be initiated. An important source of error could be the error in the frequency of the wave form synthesizer which is used as the reference source for the lock-in amplifier. We studied the problem of converting the time stamps of the data from UTC to UT1 and realized that inaccuracies in the modeling of Earth rotation parameters should be looked at in more detail.

Before the output of the Phase Plane Rotation scheme can be used to place upper bounds on the gravitational wave amplitude from PSR 0437-4715, it is necessary to study in detail

the effects of non-stationarity and non-gaussianity of the noise on the behaviour of the detection statistic. This is also now relevant for data analysis using interferometric data. Work in this direction is in progress.

ACKNOWLEDGEMENTS

The implementation of the algorithm depends crucially on the signal phase as predicted using radio observations. We thank Dr. Matthew Bailes for providing us with the relevant data and program and devoting considerable effort in adapting the data to our needs. During the completion of this work SDM was a research fellow of the Council of Scientific and Industrial Research of India. SDM thanks the LIGO project for hospitality while the paper was being completed. SDM thanks the DIST, Australia for supporting his visit to the physics department, UWA, Australia.

REFERENCES

[1] Bailes M., 1997, Private communication

[2] Blair D. G. et al., 1995, Phys. Rev. Lett., 74, 1908

[3] Brady P. R., Creighton T., Cutler C. & Schutz B., 1998, Phys. Rev., D 57, 2101

[4] Cutler C., xxx.lanl.gov e-print archive, gr-qc/9703068

[5] Dhurandhar S. V., Blair D. G. & Costa M. E., 1996, Astron. Atsrophys., 311, 1043

[6] Dhurandhar S. V. & Tinto M.,1988, MNRAS, 234, 663

[7] IERS www site, http://hpiers.obspm.fr.

[8] Ipser J. R., 1971, ApJ, 16, 175

[9] Johnston S. et al., 1993, Nature, 361, 613

[10] Kaplan G. H., NOVAS : Naval Observatory Vector Astrometry Subroutines, U. S. Naval Observatory, http://maia.usno.navy.mil.

[11] Owa S., 1986, Doctoral Dissertation, Dept. of Phy., Tokyo University

[12] Owa S. et al., 1988, in Michelson P. F. et al., eds, Proc. of the *International symposium on experimental gravitational physics* (Gangzhou, China), World Scientific, Singapore

[13] Pallotino G. V., Pizzella G, 1991, in Blair D. G., ed, *The detection of gravitational waves*, Cambridge University Press, p. 243

[14] Sandhu J. S. et al., 1997, ApJ, 478, L95

[15] In *The Explanatory Supplement to the Astronomical Almanac*, 1992, Seidelmann P. K., ed, (U.S. Naval Obs., U.S. Govt. Printing Office)

[16] Taylor J. H. & Weisberg J. M., 1989, ApJ, 345, 434.

[17] Thorne K. S., 1987, in Hawking S. W. & Israel W., eds, *300 Years of Gravitation*,

Cambridge University Press

[18] Tsubono K., 1991, in Blair D. G., ed, *The detection of gravitational waves*, Cambridge University Press, p. 226

APPENDIX A: THE SIGNAL TO NOISE RATIO FOR PHASE PLANE ROTATION

The detection statistic in PPR is the length of the final displacement of the output path from the origin. We denote it by L_T, where T is the integration period,

$$L_T = \left[\left(\int_0^T dt X'(t) \right)^2 + \left(\int_0^T Y'(t) \right)^2 \right]^{1/2} . \tag{A1}$$

$X'(t)$ and $Y'(t)$ are obtained from the lock-in outputs $X(t)$ and $Y(t)$ using Eqs. (6) and (7).

Using these equations, we can express L_T as,

$$\begin{aligned} L_T &= \left| \int_0^T dt X'(t) + i \int_0^T dt Y'(t) \right| , \\ &= \left| \int_0^T dt \left(X(t) + iY(t) \right) \exp(-i\theta_R(t)) \right| . \end{aligned} \tag{A2}$$

Now, substituting for $X(t)$ and $Y(t)$ using Eqns. (1) and (2), we get

$$\begin{aligned} L_T &= \left| \int_{-\infty}^{\infty} dt' x(t') e^{-i\omega_{\text{ref}} t'} \int_0^T dt K_L(t - t') \exp(-i\theta(t) + i\omega_{\text{ref}} t) \right| , \\ &= \left| \int_{-\infty}^{\infty} dt' x(t') e^{-i\omega_{\text{ref}} t'} \int_{-t'}^{T-t'} dx \, K_L(x) \exp\left[-i\theta(x + t') + i\omega_{\text{ref}}(x + t') \right] \right| , \\ &\simeq \left| \int_{-\infty}^{\infty} dt' x(t') e^{-i\theta(t')} \int_{-t'}^{T-t'} dx \, K_L(x) \exp\left[-i\dot{\theta}(t') x + i\omega_{\text{ref}} x \right] \right| . \end{aligned} \tag{A3}$$

Since the signal is narrow band, keeping only the first term in the Taylor series of $\theta(t)$ above is a good approximation.

Let the low pass filter $K_L(x)$ have a decay time of τ sec. Thus, if $t' < -\tau$ sec, the integral over x in Eq. (A3) would be close to zero. While if $t' \geq T$, the integral is anyway zero because of the causal nature of $K_L(x)$. The integral would have a non-negligible value only if the upper limit is restricted to $t < T - \tau$. Thus,

$$L_T = \left| \int_{-\tau}^{T-\tau} dt' x(t') e^{-i\theta(t')} \int_{-t'}^{T-t'} dx \, K_L(x) \exp\left[-i\dot{\theta}(t') x + i\omega_{\text{ref}} x \right] \right| . \tag{A4}$$

Now, the integral over x is approximately the Fourier transform of $K_L(x)$ evaluated at the frequency $\dot{\theta}(t') - \omega_{\text{ref}}$. And if $\dot{\theta}(t)$ is approximately a constant, as it would be for a sufficiently narrow band signal, this term would be an overall constant and, thus, not affect the SNR.

Thus,,

$$L_T \simeq K \left| \int_{-\tau}^{T-\tau} dt' x(t') e^{-i\theta(t')} \right| , \tag{A5}$$

where K is a constant. The remaining term is simply the correlation of $x(t)$ with the signal waveform, maximised over an initial unknown phase. Knowledge of the signal amplitude is not as important as that of the phase for detection. Note that there is no time of arrival involved here but instead there is an unknown initial phase. Thus, the SNR for PPR should be approximately the same as that of a correlation with a template wave form or, equivalently, a matched filter.

APPENDIX B: PHASE MODULATION DUE TO THE TRANSFER FUNCTION OF THE DETECTOR

The detector has a finite response time to a force acting on it. Hence, if the force has a time varying frequency, an extra phase modulation may be imposed on the detector's response. This effect was estimated in paper I by assuming that the frequency of the force changed linearly. However, a Fourier transform of the force was taken and, thus, the linear drift was implicitly assumed to be present for all time which is not true in reality.

We present here an alternative argument which is based entirely in the time domain. The transfer function of the detector for the mode f_- can be expressed as,

$$K_b(x) = \begin{cases} e^{-\beta x} \sin(\omega_- x) & , x > 0 \\ 0 & , x \leq 0 \end{cases} , \tag{B1}$$

assuming any constant phase offset to be zero and the overall amplitude to be unity, without loss of generalization. The decay time $\tau = \beta^{-1}$ of $K_b(x)$ is ~ 50 sec (paper I).

The response $\xi(t)$ of the detector to the force $F(t)$, which can be expressed using Eqs. (11), (12) and (13) as,

$$F(t) = A_s(t) \cos(\theta_s(t) + \Phi_P(t)) , \tag{B2}$$

is given by,

$$\xi(t) = \int_{-\infty}^{\infty} dt' K_b(t-t') A(t') \cos\left[\theta_s(t') + \Phi_P(t')\right] \ . \tag{B3}$$

The phase $\theta_s(t)$ arises from doppler shifts and hence can be expressed as $\theta_s(t) = \omega_p t + \omega_p d(t)$, where ω_p is the signal's centre frequency and $d(t)$ is a collection of all the doppler terms.

Taking into account the fact that t' cannot exceed t, we can express $\xi(t)$ as,

$$\begin{aligned}
\xi(t) &= \int_0^{\infty} dx\, A_s(t-x) e^{-\beta x} \sin\omega_- x \cos\left[\omega_p(t-x) + \omega_p d(t-x) + \Phi_P(t-x)\right] \ , \\
&\simeq \frac{1}{2}\cos\omega_p t \int_0^{\infty} dx\, A_s(t-x) e^{-\beta x} \cos\Delta\omega x \sin g(t-x) + \\
&\quad \frac{1}{2}\sin\omega_p t \int_0^{\infty} dx\, A_s(t-x) e^{-\beta x} \cos\Delta\omega x \cos g(t-x) + \\
&\quad \frac{1}{2}\cos\omega_p t \int_0^{\infty} dx\, A_s(t-x) e^{-\beta x} \sin\Delta\omega x \cos g(t-x) - \\
&\quad \frac{1}{2}\sin\omega_p t \int_0^{\infty} dx\, A_s(t-x) e^{-\beta x} \sin\Delta\omega x \sin g(t-x) \ ,
\end{aligned} \tag{B4}$$

where $\Delta\omega = \omega_- - \omega_p$, $g(t) = \omega_p d(t) - \Phi_P(t)$ and terms with $\omega_- + \omega_p$ inside the integrand have been neglected.

Proceeding further with the algebra, we get

$$\begin{aligned}
\xi(t) &= \frac{1}{2}\cos\omega_p t \int_0^{\infty} dx\, A_s(t-x) e^{-\beta x} \sin(\Delta\omega x + g(t-x)) + \\
&\quad \frac{1}{2}\sin\omega_p t \int_0^{\infty} dx\, A_s(t-x) e^{-\beta x} \cos(\Delta\omega x + g(t-x)) \ , \\
&= \frac{1}{2}\sqrt{f_1^2(t) + f_2^2(t)}\cos\left[\omega_p t - \tan^{-1}\frac{f_2(t)}{f_1(t)}\right] \ ,
\end{aligned} \tag{B5}$$

where,

$$f_1(t) = \int_0^{\infty} dx\, A_s(t-x) e^{-\beta x} \sin(\Delta\omega x + g(t-x)) \ , \tag{B6}$$

$$f_2(t) = \int_0^{\infty} dx\, A_s(t-x) e^{-\beta x} \cos(\Delta\omega x + g(t-x)) \ . \tag{B7}$$

Thus, the response is an amplitude and phase modulated signal with the same centre frequency of f_p as before.

Now, recall that $\beta^{-1} \sim 50$ sec. Over such an interval, the functions $A(t)$ and $g(t)$ can be taken to be approximately constant ($\dot{\Phi}_P(t) \sim 10^{-4}$ rad/sec or less and $\omega_p \dot{d}(t) \sim 7 \times 10^{-3}$ rad/sec or less). Therefore, $f_1(t)$ and $f_2(t)$ are approximately,

$$f_1(t) \simeq A_s(t)\left[\cos g(t)\int_0^\infty dx\, e^{-\beta x}\sin\Delta\omega x + \sin g(t)\int_0^\infty dx\, e^{-\beta x}\cos\Delta\omega x\right], \tag{B8}$$

$$f_2(t) \simeq A_s(t)\left[\cos g(t)\int_0^\infty dx\, e^{-\beta x}\cos\Delta\omega x - \sin g(t)\int_0^\infty dx\, e^{-\beta x}\sin\Delta\omega x\right]. \tag{B9}$$

Hence, the phase modulation term in Eq. (B5) becomes,

$$\tan^{-1}\frac{f_2(t)}{f_1(t)} \simeq g(t) + \eta(\Delta\omega)\,, \tag{B10}$$

$$\eta(\Delta\omega) = \tan^{-1}\frac{\int_0^\infty dx\, e^{-\beta x}\sin\Delta\omega x}{\int_0^\infty dx\, e^{-\beta x}\cos\Delta\omega x}\,. \tag{B11}$$

Thus, we see that in the limit of small β, the phase of the response $\xi(t)$ is altered by only $\eta(\Delta\omega)$ which is a constant if the the mode frequency f_- is kept constant.

APPENDIX C: EFFECT OF RANDOM PHASE ERRORS ON SNR IN PPR

If the phase error $\Delta\theta = \theta_S(t) - \theta_R(t)$ is a random error, where $\theta_S(t)$ denotes the actual phase of the signal in the lock-in output, then its effect on the total integrated length of the signal can be estimated as follows. Let $\Delta\theta(t)$ be a zero mean, Gaussian and stationary random process with a variance σ_θ^2 and an auto-correlation time scale τ. The total integrated length in the rotating plane, can be expressed, following the treatment given in Appendix A, as

$$L^2 = \left|\sum_{j=1}^{N} A_j e^{i\Delta\theta(t_j)}\right|^2, \tag{C1}$$

where $t_j = j\Delta$ denotes the j^{th} time sample, Δ being the sampling interval, and A_j is the amplitude $A_s(t)$ at $t = t_j$.

Thus, the relative error β between the actual squared length above and the maximum length obtainable, $\sum A_j$, would be,

$$\beta = 1 - \frac{\sum_{j,k} A_j A_k e^{i\Delta\theta(t_j)-\Delta\theta(t_k)}}{\sum_{j,k} A_j A_k}\,. \tag{C2}$$

For $|t_j - t_k| \ll \tau$, the difference $\Delta\theta(t_j) - \Delta\theta(t_k)$ can be assumed to be close to zero while for $|t_j - t_k| \gg \tau$, the random variables $\Delta\theta(t_j)$ and $\Delta\theta(t_k)$ would be statistically independent.

Now assume that τ is much smaller than the integration time T. Then the number of terms with $|t_j - t_k| \gg \tau$ would be large and will dominate the sum as compared to terms for which $|t_j - t_k| \sim \tau$. Thus, loosely speaking, we can split the numerator in Eq. (C2) as follows,

$$\epsilon \simeq 1 - \frac{\sum_j A_j^2 + 2\left(\sum_j \sum_{j<k<p} A_j A_k + \sum_j \sum_{k>p} A_j A_k \cos(\chi_{jk})\right)}{\left(\sum_j A_j\right)^2}, \tag{C3}$$

where, $p\Delta \sim \tau$ and, since $\Delta\theta(t_j)$ and $\Delta\theta(t_k)$ are statistically independent if they are far apart, $\chi_{jk} = \Delta\theta(t_j) - \Delta\theta(t_k)$ is a zero mean Gaussian random variable, distributed independently of j and k, with a variance $2\sigma_\theta^2$.

Therefore, the average value of ϵ is,

$$\langle\epsilon\rangle = \frac{(1 - \langle\cos\chi\rangle)\sum_{j=1}^{N}\sum_{k>p}^{N} A_j A_k}{\left(\sum_j A_j\right)^2}. \tag{C4}$$

Note that if $\tau \sim 0$ (the case of $\Delta\theta(t)$ being white noise), then $\langle\epsilon\rangle$ would have been larger. The ensemble average of $\cos\chi$ is easily calculated in terms of the characteristic function of the Gaussian distribution. For, $\langle\epsilon\rangle \leq 0.2$, we find that $\sigma_\theta \leq 0.03$ radians. With this relative error in the squared lengths, the error in the lengths themselves would be $\leq 10\%$. Our estimate of the error in phase, in Section VI, is well below the allowed phase error above.

FIGURES

FIG. 1. The path of 15 minutes of real data from NIOBE after being transformed according to Eqs. (6) and (7). The solid line shows that path followed by wide band noise alone. The dots show the path followed by the total noise. The circular "smearing" of the random walk is evident. The X and Y quadratures are expressed in the volts equivalent of the bar displacement ξ.

FIG. 2. The path of 15 minutes of real data when a signal wave form has been added to it prior to the rotational transformation. The noise in this figure is the same as in Fig. 1. The phase used for the rotational transform differs from that of the signal by a constant offset of 45°. Thus, the signal path grows along the 45° line and the systematic deviation of the total path along that direction is evident. The signal added is monochromatic with $f_p - f_- = 0.2$ Hz and has an r.m.s amplitude of 0.05 volts. For comparison, we show, with dots, the path followed by the noise alone.

FIG. 3. The polarization phase $\Phi_P(t;\, \rho, \psi)$, for $\psi = 0$ and several values of ρ, as a function of sidereal time. This figure is for an arbitrary epoch and spans a period of 24 hours. The solid line is for $\rho = 1$ (corresponding to an inclination angle $i = 0$), the dashed for $\rho = 0.80$ ($i = 60°$) and the dot-dashed for $\rho = 0.34$ ($i = 80°$). The angular positions used correspond to that of PSR 0437-471 and NIOBE. As the value of ρ decreases, Φ_P is confined more and more to either 0 or 2π. This is expected since, the signal becomes linearly polarized in this limit and the polarization phase should not matter.

FIG. 4. The contours of $\epsilon(\widehat{\rho}, \widehat{\psi};\, \rho_s, \psi_s)$ for a signal inclination angle $i = 30°$ and $\psi_s = 20°$. On the horizontal axis we have shown the inclination angle corresponding to $\widehat{\rho}$. It is evident that an integration with $\widehat{\rho} = 1$ and $\widehat{\psi} = 0$ is good enough to detect this signal. The best integration is, of course, the one with the same parameter values as the signal. However, the maximum at that point is very weak and not visible in this figure.

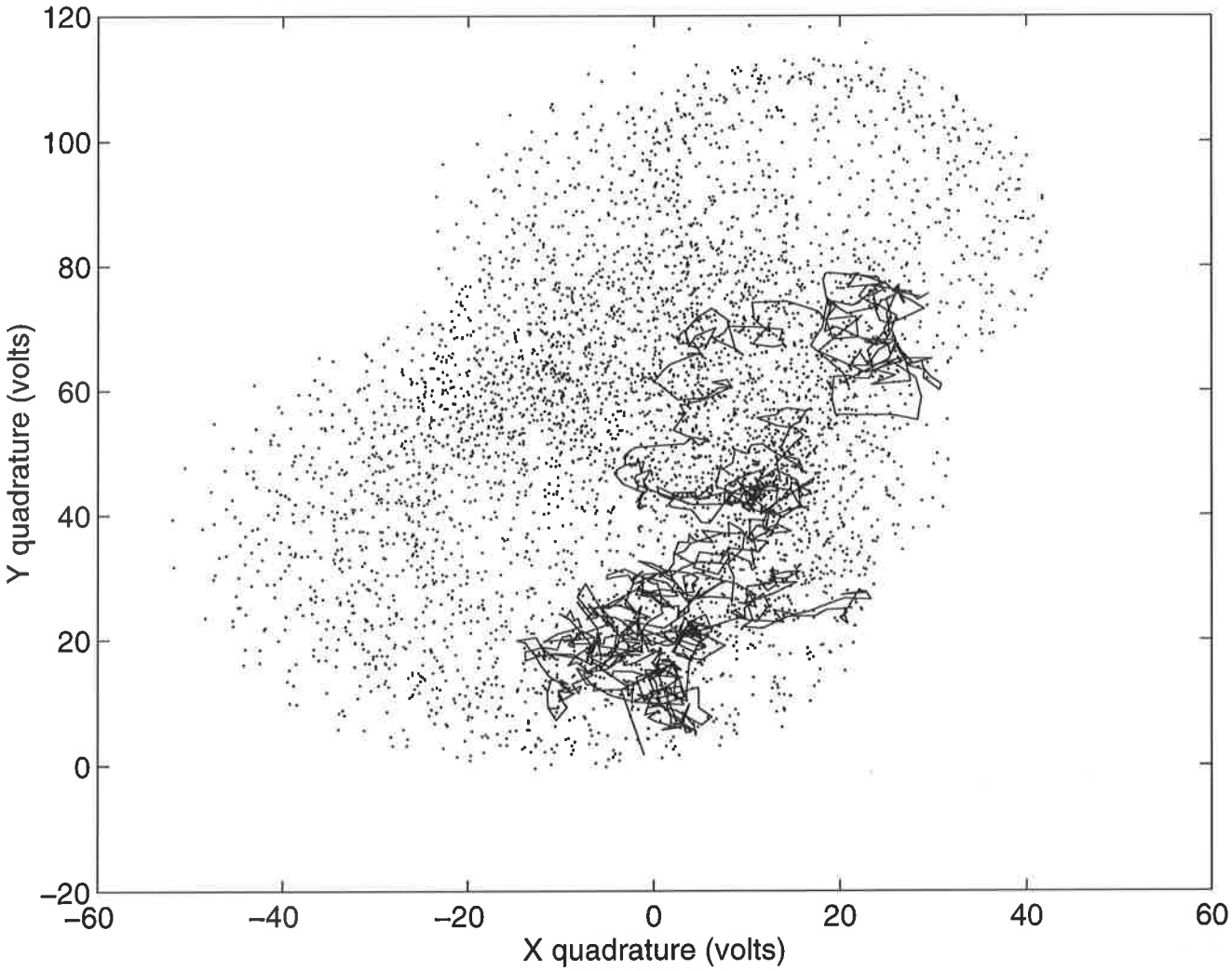
120
100
80
60
40
20
0
−20
−60
−40
−20
0
20
40
60
Y quadrature (volts)
X quadrature (volts)

Fig. 1

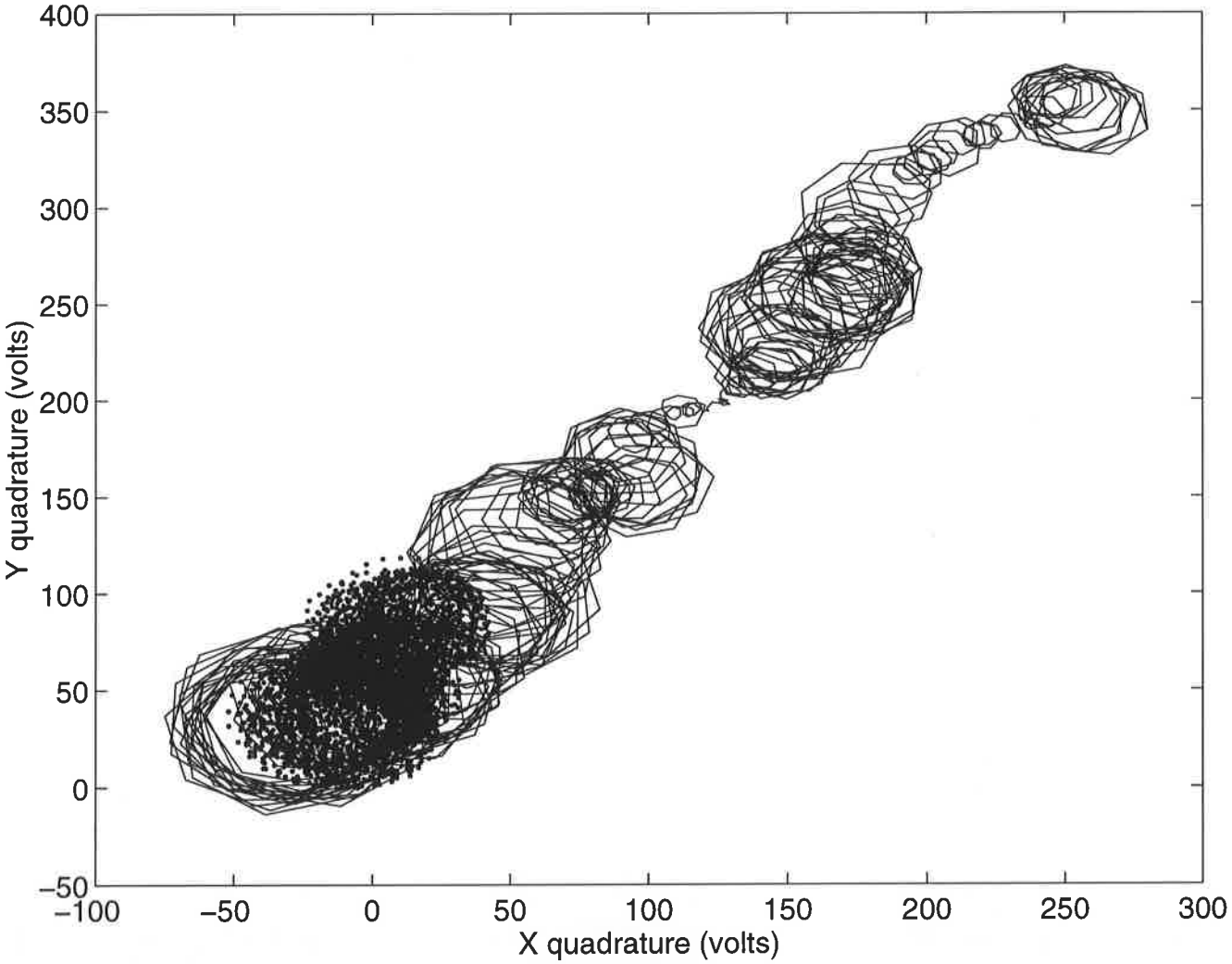
400
350
300
250
200
150
100
50
0
−50
−100
−50
0
50
100
150
200
250
300
Y quadrature (volts)
X quadrature (volts)

Fig. 2

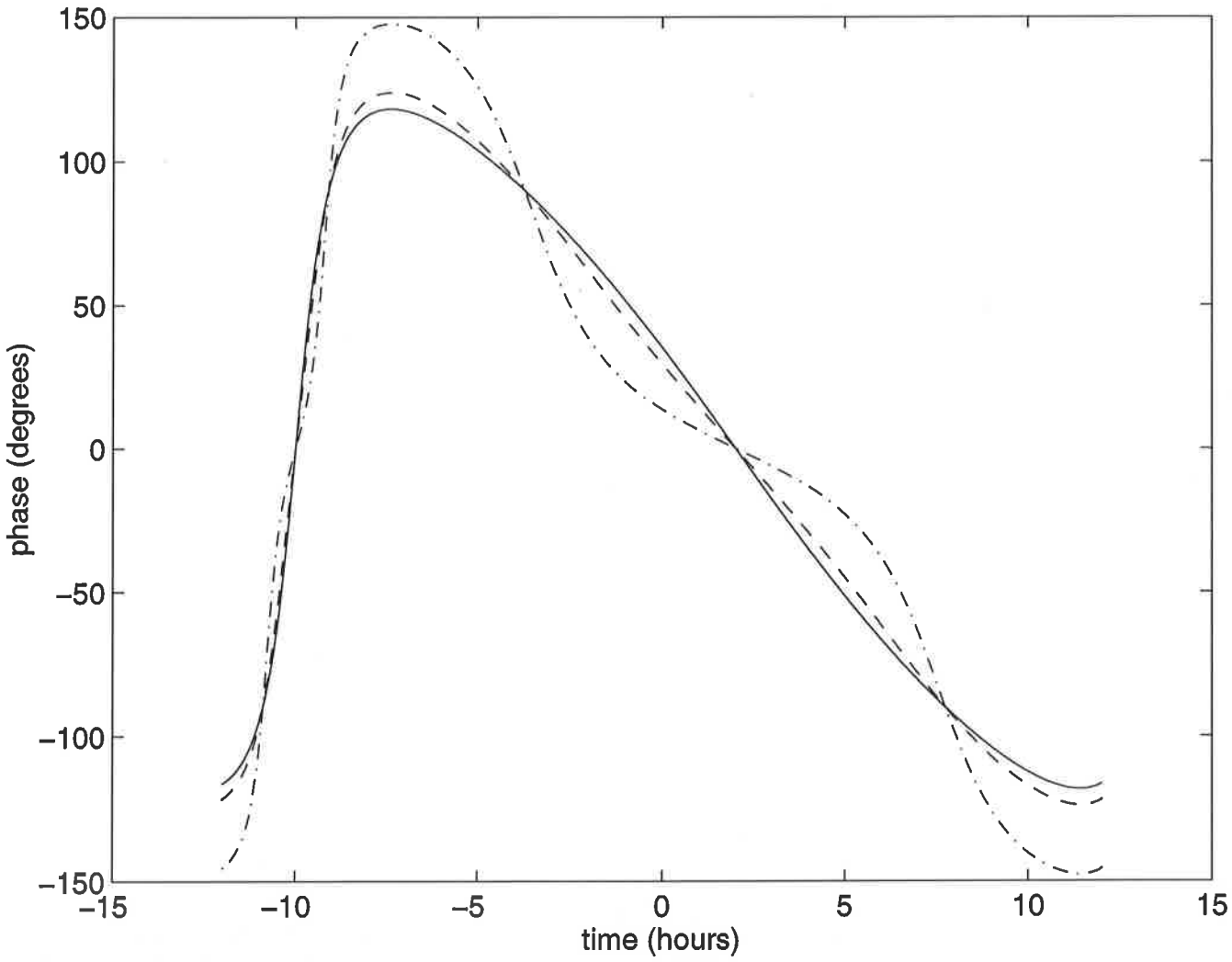

Fig. 3

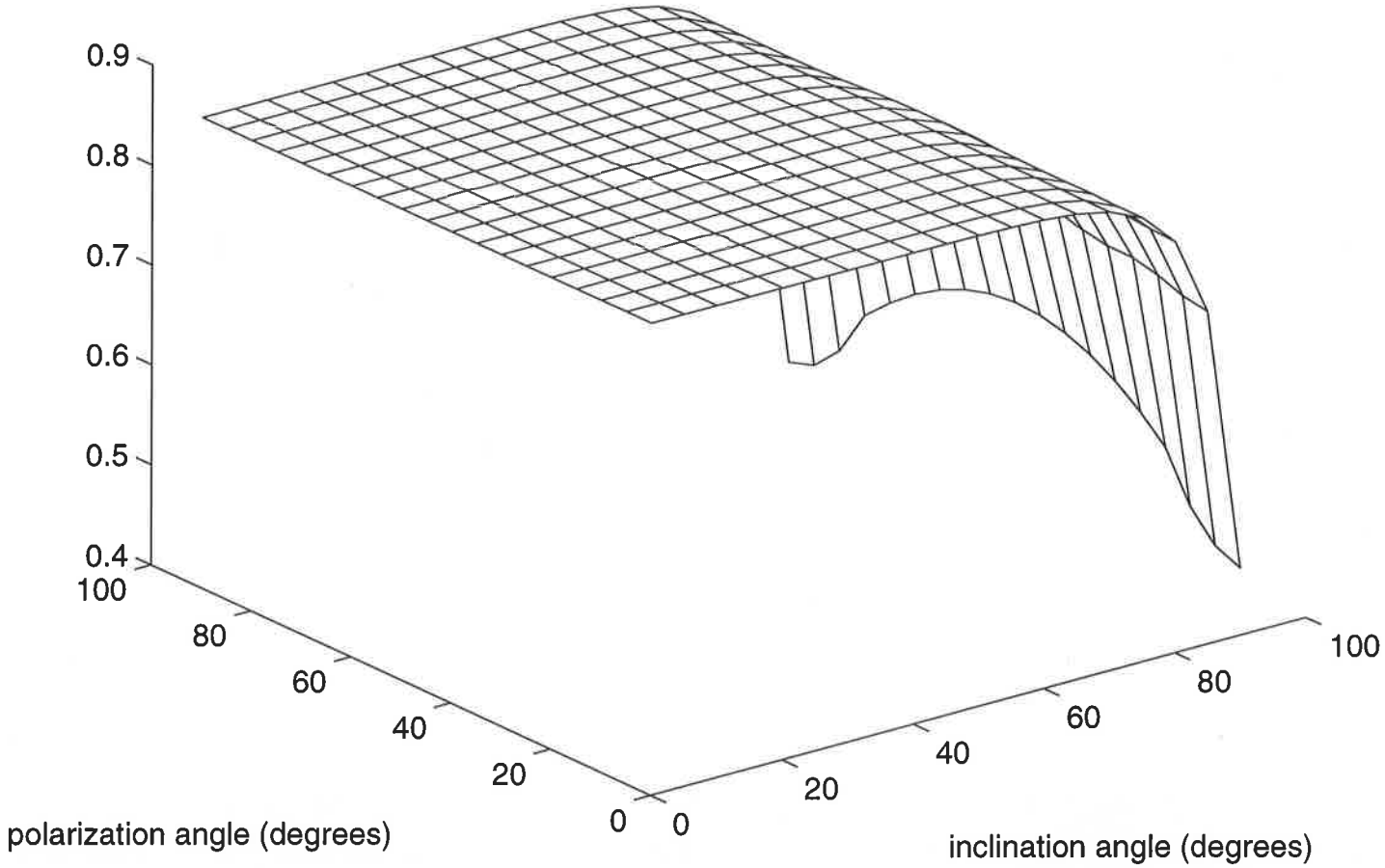
0.9
0.8
0.7
0.6
0.5
0.4
100
80
60
40
20
0
polarization angle (degrees)
0
20
40
60
80
100
inclination angle (degrees)

Fig. 4